PHYSICAL REVIEW E **69,** 046301 (2004)

Influence of a magnetic field on the Soret-effect-dominated thermal convection in ferrofluids

Andrey Ryskin and Harald Pleiner
Max-Planck-Institut für Polymerforschung, D 55021 Mainz, Germany
(Received 17 November 2003)

We investigate theoretically the influence of a magnetic field on the growth of convective rolls in a slab of ferrofluid subject to a vertical temperature gradient. Due to the pronounced Soret effect of these materials in combination with a considerable solutal expansion, a dynamic description as a binary mixture is appropriate. We first derive a comprehensive set of magnetic field effects in the statics and dynamics of binary mixtures. Among those, the two prominent ones, the Kelvin force and magnetophoresis, are studied in detail with respect to their influence on the thermal convection behavior. The main difference from the case without an external field rests in the importance of the boundary layers, which influence the bulk problem through the magnetic boundary conditions. We discuss an analytical approximate solution and compare it with a numerical multimode expansion.

PACS numbers: 47.20.-k, 44.27.+g, 75.50.Mm DOI: 10.1103/PhysRevE.69.046301

I. INTRODUCTION

Ferrofluids are dispersions of heavy solid ferromagnetic grains suspended in a carrier liquid [1]. With a typical diameter of 10 nm the particles are quite large on molecular length scales, resulting in an extremely small particle mobility [2]. This leads to a situation where demixing effects take place on time scales far beyond any reasonable observation time. On the other hand, ferrofluids are characterized by a large thermodiffusive or Soret effect. As a result of the joint action of thermal and solutal buoyancy forces (e.g., for a cyclohexane carrier), the critical Rayleigh number Ra_c for the onset of convection is dramatically reduced as compared to the pure fluid reference value $Ra_c^0 = 1708$. However, Ra_c is experimentally inaccessible due to the extremely slow growth of convection patterns, requiring extremely large observation times. It has been shown recently [3] that, starting from an initial motionless configuration with a uniform concentration distribution, convective perturbations grow even at Rayleigh numbers well below the threshold Ra_c^0 of pure fluid convection. This happens within a time small compared to the creeping solutal diffusion time, but almost as fast as pure-fluid convection does at $Ra > Ra_c^0$.

Here we investigate the influence of an external magnetic field on this convection scenario for positive separation ratio ψ. We first (Sec. II) review the hydrodynamic equations for binary mixtures in the presence of an external magnetic field. We assume the magnetization to be already relaxed to its equilibrium value on the time scales under consideration. The magnetic field effects then come basically in two different varieties. First the Maxwell stress, which can be written as a Kelvin force in the momentum conservation law (the Navier-Stokes equation), and second the temperature and concentration dependence of the magnetic susceptibility in the statics that gives rise to a field dependence of heat and concentration currents (magnetophoresis). If a temperature gradient is applied across the ferrofluid layer, the experimentally relevant convection-free ground state is not the true stationary state with a linear concentration profile, but the purely conducting state with a constant concentration (apart from a very thin boundary region) [3] and a linear magnetic field profile (Sec. III). The stability of this ground state is investigated by solving approximately the nonlinear dynamic equations for deviations from it. Within the usual Boussinesq approximation five magnetic field effects, characterized by dimensionless numbers proportional to the field strength squared, show up in the equations and boundary conditions (Sec. IV). Among them, M_1, the strength of the magnetic relative to the buoyancy force, and M_2, the magnetophoretic number, seem to be the most important.

To solve the system of equations we first set up a multimode Galerkin description (Sec. V), where in particular for the concentration and the magnetic potential the inclusion of many modes turn out to be essential. An approximate ansatz is solved analytically (Sec. VI). Here the necessity of dealing carefully with the boundary layer profiles of concentration and magnetic potential (Appendices A and B) becomes obvious. This approximate analytical solution is compared with the numerical Galerkin results, in particular with respect to the influence of the Kelvin force (M_1) in Sec. VII. The role of magnetophoresis (M_2) on the instability behavior is discussed in Sec. VIII.

II. BASIC EQUATIONS

Ferrofluids can be treated as a superparamagnetic continuum [1] that consists of two different nonreacting materials (binary mixture). An external magnetic field easily induces a considerable magnetization in the fluid.

This magnetization is in principle a dynamic degree of freedom. However, it relaxes rather quickly to its equilibrium value and orientation given by the Maxwell field $\boldsymbol{H}$. Thus, for the time scales of interest for the convection problem we can always assume $\boldsymbol{M} = \boldsymbol{M}(\boldsymbol{H})$. Here we review the hydrodynamic equations for a binary mixture subject to an external static magnetic field and bring them into a form suitable for the convection problem. The hydrodynamics is most easily set up by using those quantities as dynamic variables that are related to local conservation laws [4]. In our case, those are the density ρ, momentum density $\rho\boldsymbol{v}$, entropy density σ and concentration C (of magnetic particles), while the chemical potential μ, the velocity $\boldsymbol{v}$, the temperature T, and the relative chemical potential μ_c are taken as their respective thermodynamic conjugate quantities. The dynamic equations read [4]

$$\dot{\rho} + \mathrm{div}(\rho\boldsymbol{v}) = 0 \tag{1}$$

$$\dot{\sigma} + \boldsymbol{v}\cdot\boldsymbol{\nabla}\sigma = \boldsymbol{\nabla}\cdot\tilde{\kappa}\,\boldsymbol{\nabla}T + \boldsymbol{\nabla}\cdot\tilde{D}_T\boldsymbol{\nabla}(\frac{\mu_c}{\rho}) + \frac{R}{T} \tag{2}$$

$$\rho(\dot{C} + \boldsymbol{v}\cdot\boldsymbol{\nabla}C) = \boldsymbol{\nabla}\cdot D\,\boldsymbol{\nabla}(\frac{\mu_c}{\rho}) + \boldsymbol{\nabla}\cdot\tilde{D}_T\boldsymbol{\nabla}T \tag{3}$$

$$\rho(\dot{v}_i + v_j\nabla_j v_i) + \nabla_i p = \nabla_j\rho\,\nu_{ijkl}\nabla_l v_k + M_j\nabla_i H_j + \rho g_i^E \tag{4}$$

while the magnetic field $\boldsymbol{H}$ and induction $\boldsymbol{B}$ are determined by Maxwell's equations, which read in the static and nonconducting case

$$\begin{aligned} \nabla\cdot\boldsymbol{B} &= 0 && (5)\\ \nabla\times\boldsymbol{H} &= 0 && (6) \end{aligned}$$

Generally, due to the presence of an external field, the transport coefficients $\tilde{\kappa}$, $\tilde{D}_T$, and D should be written as tensors of the form $D_{ij} = D\delta_{ij} + D^R\epsilon_{ijk}H_k$ with Hall- or Righi-Leduc-type contributions [5]. However, those terms are inoperative for the geometry considered below. The same is true for similar linear field contributions to the viscosity tensor [5], which can qualitatively change the patterns in the Benard instability in ferronematics [6], but do not contribute here.

As usual for convection problems we apply the Boussinesq approximation implying incompressibility div$\boldsymbol{v} = 0$, neglect of the dissipation function R in Eq.(2), and taking all material parameters as constants except for the density in the gravity force ρg_i^E. The Navier-Stokes equation (4) has been written in a form where the Kelvin force, with $\boldsymbol{M} = \boldsymbol{B} - \boldsymbol{H}$ [7], shows up on the right hand side. Due to the incompressibility approximation the pressure p is no longer a thermodynamic variable and its dependence on the magnetic field is irrelevant. It is only an auxillary quantity that ensures the incompressibility condition for all times, but it is not needed in the following. As discussed above, the magnetization is not a dynamic degree of freedom.

To close the system of equations we need the static relations between the conjugate quantities and the variables. Standard procedure gives [4]

$$\begin{aligned} \delta T &= \frac{T}{c_V}\delta\sigma + \beta_c\,\delta C && (7)\\ \delta\mu_c &= \gamma\,\delta C + \beta_c\,\delta\sigma && (8)\\ \delta\boldsymbol{B} &= (1+\chi)\,\delta\boldsymbol{H} && (9) \end{aligned}$$

derived from an energy density

$$\epsilon = \epsilon_0 + \frac{T}{2c_V}(\delta\sigma)^2 + \beta_c(\delta\sigma)(\delta C) + \frac{\tilde{\gamma}}{2}(\delta C)^2 + \frac{1}{2}(1+\chi)(\delta\boldsymbol{H})^2 \tag{10}$$

In this form the static equations generally are not suitable for ferrofluids, since the magnetic susceptibility χ depends considerably on the concentration (of the magnetic particles), the temperature and the external field. Switching to the temperature as variable by a Legendre transformation, $\tilde{\epsilon} = \epsilon - (\delta\sigma)(\delta T)$, and taking $\chi = \chi(T, C, H^2)$ we get

$$\delta\sigma = \frac{c_H}{T}\delta T - \frac{\beta_H c_V}{T}\delta C + \chi_T\,\boldsymbol{H_0}\cdot\delta\boldsymbol{H} \tag{11}$$

$$\delta\mu_c = \gamma_H\,\delta C + \frac{\beta_H c_V}{T}\delta T + \chi_c\,\boldsymbol{H_0}\cdot\delta\boldsymbol{H} \tag{12}$$

$$\delta\boldsymbol{B} = (1+\chi_0)\,\delta\boldsymbol{H} + \boldsymbol{H}_0\,(\chi_T\,\delta T + \chi_c\,\delta C + \chi_H\boldsymbol{H_0}\cdot\delta\boldsymbol{H}) \tag{13}$$

where χ_0 is the (constant) magnetic susceptibility taken at the equilibrium field $\boldsymbol{H}_0$, equilibrium temperature T_0, and equilibrium concentration C_0. It is assumed to be a known function of H_0^2. Up to second order derivatives of χ we have

$$\begin{aligned} c_H &= c_V - \frac{T_0}{2}H_0^2\,\frac{\partial^2\chi}{\partial T^2} && (14)\\ \beta_H &= \beta_c + \frac{T_0}{2c_V}H_0^2\,\frac{\partial^2\chi}{\partial T\,\partial C} && (15)\\ \gamma_H &= \tilde{\gamma} - \frac{\beta^2 c_V}{T_0} + \frac{1}{2}H_0^2\,\frac{\partial^2\chi}{\partial C^2} && (16)\\ \chi_T &= \frac{\partial\chi}{\partial T} + H_0^2\frac{\partial^2\chi}{\partial T\,\partial H^2} && (17)\\ \chi_c &= \frac{\partial\chi}{\partial C} + H_0^2\frac{\partial^2\chi}{\partial C\,\partial H^2} && (18)\\ \chi_H &= 4\frac{\partial\chi}{\partial H^2} + 2H_0^2\frac{\partial^2\chi}{(\partial H^2)^2} && (19) \end{aligned}$$

implying an H_0^2 dependence of the usual static susceptibilities. In principle, the static susceptibilities can be arbitrary functions of H_0^2. Thermodynamic stability (positivity of the energy functional) requires the following positivity conditions:

$$c_H > 0, \qquad \gamma_H > 0, \qquad 1+\chi_0 > 0, \qquad \bar{\epsilon} > 0,$$

$$c_H\gamma_H > \left(\frac{\beta_H c_V}{T}\right)^2, \quad c_H\bar{\epsilon} > \chi_T^2 H_0^2, \quad \gamma_H\bar{\epsilon} > \chi_c^2 H_0^2, \tag{20}$$

with $\bar{\epsilon} = 1 + \chi_0 + \chi_H H_0^2$ [8].

In order to retain the buoyancy force, the temperature and concentration dependence of the density has to be kept in the gravity force, which can be written as

$$\rho g_i^E = -g_E \rho_0 (1 + \alpha_\theta\, \delta T - \alpha_c\, \delta C - \alpha_H \boldsymbol{H}_0 \cdot \delta\boldsymbol{H})\, \delta_{iz}, \tag{21}$$

taking the z direction as the vertical one. The magnetic field contribution to the buoyancy force due to deviations of the magnetic field from its constant and homogeneous equilibrium value has been introduced for completeness.

Combining the static and dynamic part, the basic equations are

$$\mathrm{div}\boldsymbol{v} = 0 \tag{22}$$

$$\frac{c_H}{T_0}\left(\frac{\partial}{\partial t} + \boldsymbol{v}\cdot\boldsymbol{\nabla}\right)T + \chi_T \boldsymbol{H}_0 \cdot \left(\frac{\partial}{\partial t} + \boldsymbol{v}\cdot\boldsymbol{\nabla}\right)\boldsymbol{H} = \bar{\kappa}\Delta T + \bar{D}_T\frac{\gamma_H}{\rho_0}\Delta C + \bar{D}_T\frac{\chi_c}{\rho_0}\boldsymbol{H}_0\cdot\Delta\boldsymbol{H} \tag{23}$$

$$\rho_0\left(\frac{\partial}{\partial t} + \boldsymbol{v}\cdot\boldsymbol{\nabla}\right)C = D\frac{\gamma_H}{\rho_0}\Delta C + \bar{D}_T\Delta T + D\frac{\chi_c}{\rho_0}\boldsymbol{H}_0\cdot\Delta\boldsymbol{H} \tag{24}$$

$$\begin{aligned}\left(\frac{\partial}{\partial t} + \boldsymbol{v}\cdot\boldsymbol{\nabla}\right)(\mathrm{curl}\boldsymbol{v})_i - \nu\Delta(\mathrm{curl}\boldsymbol{v})_i \\ = \epsilon_{ikz} g_E(\alpha_\theta \nabla_k T + \alpha_c\nabla_k C + \alpha_H \boldsymbol{H}_0\cdot\nabla_k\boldsymbol{H}) \\ + \frac{1}{\rho_0}\epsilon_{ikl}(\boldsymbol{H}_0\cdot\nabla_l\boldsymbol{H})\,(\chi_T\nabla_k T + \chi_c\nabla_k C)\end{aligned} \tag{25}$$

with $\Delta = \boldsymbol{\nabla}^2$ and

$$\bar{\kappa} = \tilde{\kappa} + 2\tilde{D}_T\frac{\beta_H c_V}{\rho_0 T_0} + D\left(\frac{\beta_H c_V}{\rho_0 T_0}\right)^2, \tag{26}$$

$$\bar{D}_T = \tilde{D}_T + D\,\frac{\beta_H c_V}{\rho_0 T_0} \tag{27}$$

The temperature conduction coefficient is $\kappa \equiv \bar{\kappa}T_0/c_H$, the diffusion coeffient $D_c \equiv D\gamma_H/\rho_0^2$, the Soret coefficient is $D_s \equiv \bar{D}_T/\rho_0$, the Dufour coefficient is $D_f \equiv \bar{D}_T\gamma_H T_0/(\rho_0 c_H)$, and ν is the dynamic shear viscosity.

The boundaries are assumed to be ideal thermal conductors; thus the temperature of the fluid at the boundaries is identical to the applied temperature. Note that in real experimental situations the finite heat conductivity of the boundaries could lead to some noticeable effects [9], but we are not going to discuss these effects in what follows. For the velocity field we assume "rigid" boundary conditions, while for the magnetic field and magnetic induction the usual continuity conditions apply:

$$\hat{\boldsymbol{n}}\cdot(\boldsymbol{B}_{int} - \boldsymbol{B}_{ext}) = 0, \tag{28}$$

$$\hat{\boldsymbol{n}}\times(\boldsymbol{H}_{int} - \boldsymbol{H}_{ext}) = 0, \tag{29}$$

with $\hat{\boldsymbol{n}}$ the normal to the boundaries. For the concentration of the ferroparticles we have the impermeability condition, i.e., no flux on the boundaries is allowed,

$$D\gamma_H\, \hat{\boldsymbol{n}}\cdot\boldsymbol{\nabla}C + \rho_0\bar{D}_T\, \hat{\boldsymbol{n}}\cdot\boldsymbol{\nabla}T + D\chi_c\, \boldsymbol{H}_0\cdot(\hat{\boldsymbol{n}}\cdot\boldsymbol{\nabla})\boldsymbol{H} = 0. \tag{30}$$

III. HEAT CONDUCTING STATE

For a layer of thickness d with prescribed temperatures T_0 and T_1 at the boundaries $z = 0$ and d, respectively, and with infinite lateral dimensions, the pure conductive state is easily found. The concentration and the magnetic field show linear z deviations from the equilibrium values, given by the boundary conditions (28), (30):

$$\mathbf{v} = 0, \tag{31}$$

$$T = T_0 - \beta z, \tag{32}$$

$$C = C_0 + \frac{D_1}{D_2}\beta z, \tag{33}$$

$$H_z = H_0\left(1 + \frac{D\gamma_H\chi_T - \rho_0\chi_c\bar{D}_T}{\bar{\epsilon}D_2}\beta z\right), \tag{34}$$

where $\beta = (T_0 - T_1)/d$, H_0 is related to the strength of the magnetic field outside the layer $\boldsymbol{H}_0^{ext}$ by the expression $\boldsymbol{H}_0^{ext} = [H_0 + M(H_0)]\hat{\boldsymbol{e}}_z)$, $D_1 = \rho_0\bar{D}_T(1 + O(H_0^2))$, and $D_2 = D\gamma_H(1 + O(H_0^2))$. However, as was the case in thermal convection without a magnetic field [3], to reach this conductive state one needs to wait untill the very slow process of concentration diffusion has equilibrated. A estimated in [3] this takes as long as a week under the usual experimental conditions. For this reason we consider the stability not of the state given by Eq. (33) but of the quasistationary state when the temperature field Eq. (32) is equilibrated, but the concentration field is still homogeneous except for very thin boundary layers near the boundaries. This situation is similar to that without a magnetic field considered in [3]. With this approximation the quasi-stationary state reads

$$\mathbf{v} = 0, \tag{35}$$

$$T = T_0 - \beta z, \tag{36}$$

$$C = C_0, \tag{37}$$

$$H_z = H_0\left(1 + \frac{\chi_T}{\bar{\epsilon}}\beta z\right). \tag{38}$$

This state is not a solution of the boundary condition (30), but it gives a good approximation to the solution for experimentally relevant times.

IV. DEVIATIONS FROM THE CONDUCTING STATE

The next step is to write the equations for the deviations from the heat conducting state (35)-(38). To do so in dimensionless form we introduce the characteristic scales d for length, d^2/κ for time (with $\kappa = \bar{\kappa}T_0/c_H$), βd

for temperature, $\beta\bar{D}_T\rho_0 d/(D\gamma_H)$ for concentration, κ/d for velocity, and $\beta d\chi_T H_0/\bar{\epsilon}$ (with $\bar{\epsilon} \equiv 1 + \chi_0 + \chi_H H_0^2$) for magnetic field. For the deviations from the magnetic field (38) a scalar potential can be introduced $\boldsymbol{H} = H_z\hat{\boldsymbol{e}}_z - \boldsymbol{\nabla}\phi$, while the magnetic potential outside the layer is defined by $\boldsymbol{H}_{ext} = \boldsymbol{H}_0^{ext} - \boldsymbol{\nabla}\phi_e$. The deviation of the temperature from Eq. (36) is θ. Then Eqs. (5) and (22)-(25) lead to

$$\nabla \cdot \mathbf{v} = 0 \tag{39}$$

$$\left[\frac{\partial}{\partial t} + (\mathbf{v}\cdot\nabla)\right](\theta - M_4\nabla_z\phi)$$
$$= w(1 - M_4) + \Delta\theta + F\Delta(C - M_2\nabla_z\phi) \tag{40}$$

$$\left[\frac{\partial}{\partial t} + (\mathbf{v}\cdot\nabla)\right] C = L\Delta(\theta + C - M_2\nabla_z\phi) \tag{41}$$

$$\begin{aligned}\frac{1}{Pr}\left[\frac{\partial}{\partial t} + (\mathbf{v}\cdot\nabla)\right](curl\mathbf{v})_i - \Delta(curl\mathbf{v})_i \\ = Ra\,\epsilon_{ikz}\nabla_k[(1 + M_1)\,\theta - (\psi + \psi_m M_1)\,C \\ +(M_5 - M_1)\nabla_z\phi] \\ -Ra\,M_1\,\epsilon_{ikl}(\nabla_l\nabla_z\phi)\nabla_k\,(\theta - \psi_m C)\end{aligned} \tag{42}$$

$$(\nabla_z^2 + M_3\Delta_\perp)\phi = \nabla_z(\theta - \psi_m C) \tag{43}$$

$$\Delta\phi_e = 0 \tag{44}$$

where w is the z component of the velocity. The transverse Laplacian $\Delta_\perp = \Delta - \nabla_z^2$. The nondimensional parameters introduced here are: the Rayleigh number $Ra = \alpha_\theta\beta g_E d^4/(\kappa\nu)$, the Prandtl number $Pr = \nu/\kappa$, the separation ratio $\psi = \alpha_c\rho_0\bar{D}_T/(\alpha_\theta\gamma_H D)$, the magnetic separation ratio $\psi_m = -\chi_c\rho_0\bar{D}_T/(\chi_T\gamma_H D)$, the Lewis number $L = \gamma_H c_H D/(\rho_0^2\bar{\kappa}T_0) = D_c/\kappa$, the strength of the magnetic force relative to buoyancy $M_1 = \beta\chi_T^2 H_0^2/(\rho_0 g_E\alpha_\theta\bar{\epsilon})$, the magnetophoretic number $M_2 = D\chi_c\chi_T H_0^2/(\rho_0\bar{D}_T\bar{\epsilon})$, the nonlinearity of magnetization $M_3 = (1+\chi_0)/\bar{\epsilon} \approx 1 - \chi_H H_0^2/(1+\chi_0)$, the relative strength of the temperature dependence of the magnetic susceptibility $M_4 = \chi_T^2 H_0^2 T_0/(c_H\bar{\epsilon})$, the ratio of magnetic to thermal buoyancy $M_5 = \alpha_H\chi_T H_0^2/(\alpha_\theta\bar{\epsilon})$, and the Dufour number $F = \bar{D}_T^2/(D\bar{\kappa}) = D_s D_f/(\kappa D_c)$. The stability conditions (20) require $M_4 < 1$ and $M_2\psi_m > -1$.

According to our choice of "rigid" and ideally conducting boundaries, the boundary conditions for the deviations from the conducting state read

$$\theta\,|_{z=\pm\frac{1}{2}} = 0 \tag{45}$$
$$w\,|_{z=\pm\frac{1}{2}} = 0 \tag{46}$$
$$\nabla_z w\,|_{z=\pm\frac{1}{2}} = 0 \tag{47}$$
$$\nabla_z(\theta + C - M_2\nabla_z\phi)\,|_{z=\pm\frac{1}{2}} = 1 - M_2 \tag{48}$$

and the magnetic boundary conditions (28) and (29) are

$$\bar{\epsilon}(\nabla_z\phi + \psi_m C) - \nabla_z\phi_e\,|_{z=\pm\frac{1}{2}} = 0 \tag{49}$$
$$\boldsymbol{\nabla}_\perp\phi - \boldsymbol{\nabla}_\perp\phi_e\,|_{z=\pm\frac{1}{2}} = 0 \tag{50}$$

These boundary conditions close the problem of finding the fields $\mathbf{v}, \theta, C$, ϕ, and ϕ_e.

V. SIMPLE GALERKIN SOLUTION

The set of equations derived in the previous section is still unnecessarily complicated. We will simplify it first by neglecting the Dufour effect, i.e., putting $F = 0$, as is usually done for any liquid. Second, we discard M_4, which is a common simplification in the description of instabilities in ferrofluids [10, 11]. Since M_4 is not related to concentration effects, which we are interested in here, we expect not to loose any reasonable aspect of the problem under consideration. The same is true for the coefficient M_5. It may be important in a situation where the concentration dynamics is not considered at all, since in that case it is the only nonthermal contribution to buoyancy. Thus, we are left with 3 magnetic field dependent effects characterized by $M_{1,2,3}$. The first denotes the influence of the Kelvin force and is expected to have the dominant influence on the convection behavior. The second effect, which we will treat in a second step, constitutes magnetophoresis, the dependence of the concentration current on the magnetic field. The third effect is due to the nonlinearity of the magnetization as a function of the Maxwell field. Generally, M_3 is rather close to 1 (the linear case $\chi = const.$ or $\boldsymbol{M} \sim \boldsymbol{H}$), since the dependence on M_3 is rather weak we always take $M_3 = 1.1$. The parameter ψ is known to be between 10 and 100 and can have negative or positive sign depending on the ferrofluid used [12]. Here we consider only the case of a positive value of ψ. Making a simple estimate, we find that the value ψ_m has the same sign and is of the same order of magnitude as ψ for typical ferrofluids.

The boundary value problem obtained in this way is still too complicated to allow a simple analytical (one-mode solution), even if unrealistic "free" boundary conditions are used for the velocity field. This is due to the magnetic boundary condition (49) which involves the concentration. Sacrificing this condition, however, would change the bifurcation scenario qualitatively, rendering such an analytical solution worthless. Instead, any realistic treatment has to take into account the boundary layer fields of concentration and magnetic field potential. We will do this analytically later on in a simplified way guided by the numerical results, which we will derive first using the Galerkin technique. To that end we make the following ansatz of a two-dimensional pattern, which is laterally (in the x direction) infinite and periodic with wave number k. These equations describe two-dimensional convection in the form of parallel rolls along the y axis in an infinite slab of thickness 1. In the lateral direction we will restrict ourselves to the fundamental mode, neglecting higher harmonics, while in the z direction (across the layer) a multimode description will be used where necessary. We have

$$\begin{aligned} C\,(x,z,t)-C_0 &= c_0(z,t)+c_1(z,t)\cos kx, && (51)\\ \theta(x,z,t) &= \theta_0\,(z,t)+\theta_1\,(z,t)\cos kx, && (52)\\ v_x(x,z,t) &= -(1/k)\nabla_z w_1(z,t)\sin kx, && (53)\\ v_z(x,z,t) &= w_1(z,t)\cos kx, && (54)\\ \phi\,(x,z,t) &= \phi_0\,(z,t)+\phi_1\,(z,t)\cos kx. && (55)\end{aligned}$$

with incompressibility already built in. We can get rid of the external potential ϕ_e by solving Eq.(44) explicitly. The solutions that vanish at $z=\pm\infty$ and satisfy the boundary condition (50) are $\phi_e=\exp(\frac{k}{2})\exp(\mp kz)\phi_1(z{=}\pm\frac{1}{2},t)\cos kx$ for the ranges $\{1/2,\infty\}$ and $\{-1/2,-\infty\}$, respectively. The boundary conditions (49) can then be written in final form

$$\bar\epsilon(\nabla_z\phi_1+\psi_m c_1)\pm k\phi_1|_{z=\pm\frac{1}{2}} = 0 \qquad (56)$$

$$\nabla_z\phi_0+\psi_m c_0|_{z=\pm\frac{1}{2}} = 0 \qquad (57)$$

Substituting Eqs. (51)-(55) into the nonlinear equations of motion (39)-(43) and sorting for different lateral dependencies yields the following system of equations

$$\begin{aligned} &\frac{1}{Pr}\partial_t\left(\nabla_z^2-k^2\right)w_1-(\nabla_z^2-k^2)^2 w_1\\ &= -Ra\,k^2\left[(1+M_1)\theta_1-(\psi+M_1\psi_m)c_1-M_1\nabla_z\phi_1\right]\\ &\quad +Ra\,M_1k^2\left(\theta_1-\psi_m c_1-\nabla_z\phi_1\right)\nabla_z\left(\theta_0-\psi_m\,c_0\right) \qquad (58)\end{aligned}$$

$$\partial_t c_0+\tfrac{1}{2}\nabla_z\left(w_1c_1\right)=L\nabla_z^2\left[(1+M_2\psi_m)c_0+(1-M_2)\theta_0\right], \qquad (59)$$

$$\partial_t c_1+w_1\nabla_z c_0=L\left(\nabla_z^2-k^2\right)\left(c_1+\theta_1-M_2\nabla_z\,\phi_1\right), \qquad (60)$$

$$\partial_t\,\theta_0+\tfrac{1}{2}\nabla_z\left(w_1\theta_1\right)=\nabla_z^2\,\theta_0, \qquad (61)$$

$$\partial_t\,\theta_1+w_1\nabla_z\,\theta_0=-w_1+\left(\nabla_z^2-k^2\right)\theta_1, \qquad (62)$$

$$\left(\nabla_z^2-M_3k^2\right)\phi_1=\nabla_z\left(\theta_1-\psi_m c_1\right), \qquad (63)$$

The field ϕ_0 has already been eliminated with the help of $\nabla_z^2\phi_0=\nabla_z(\theta_0-\psi_m c_0)$. This has also been used to write the remaining boundary conditions as

$$\begin{aligned} \nabla_z(c_1+\theta_1-M_2\nabla_z\phi_1)|_{z=\pm1/2} &= 0, && (64)\\ \nabla_z((1+M_2\psi_m)c_0+(1-M_2)\theta_0)|_{z=\pm1/2} &= 1-M_2 && (65)\\ \theta_1|_{z=\pm1/2}=\theta_0|_{z=\pm1/2} &= 0, && (66)\\ w_1|_{z=\pm1/2}=\nabla_z w_1|_{z=\pm1/2} &= 0, && (67)\end{aligned}$$

To solve this boundary value problem we adopt vertical profiles w_1, θ_0, θ_1, c_0, c_1, and ϕ_1 in the form

$$\begin{aligned} w_1(z,t) &= A(t)\cos^2(\pi z)\,, && (68)\\ \theta_1(z,t) &= B(t)\cos\pi z, && (69)\\ \theta_0(z,t) &= G(t)\sin 2\pi z, && (70)\\ c_0(z,t) &= \frac{1-M_2}{1+\psi_m M_2}[z-\theta_0(z,t)]\\ &\quad+\sum_{n=0}^{n=N}a_n(t)\sin\left(2n+1\right)\pi z, && (71)\\ c_1(z,t) &= -\theta_1(z,t)+\sum_{n=0}^{n=N}b_n(t)\cos 2n\pi z, && (72)\\ \phi_1(z,t) &= A_0(t)\,z+\sum_{n=0}^{n=N_1}\frac{A_n(t)\sin 2\pi nz}{2\pi n} && (73)\end{aligned}$$

which satisfy the boundary conditions (56),(64)-(67) identically, if $A_0(2+k)+\sum_{n=1}^{N_1}(-)^nA_n+\psi_m\sum_{n=1}^{N}(-)^nb_n=0$ is chosen.

We point out that for $\psi=0$ and $\psi_m=0$ the concentration fields decouple from temperature and velocity. This reduces Eqs. (68)-(70) in the absence of the magnetic field to the three-mode model introduced by Lorenz [13] to mimic the dynamics of convective rolls in single-component Rayleigh-Bénard convection. In the case of finite magnetic field this is a somewhat modified Lorenz model for a magnetic fluid [14]. At nonzero ψ and ψ_m, convection is modified by the concentration field but we can adopt the above few-mode expansion for temperature and velocity [3] without modifications, because the diffusivities for heat and momentum are large enough to prevent the appearance of strong gradients. By way of contrast, owing to the small Lewis number, the concentration field does build up steep boundary layers, which we account for by a N-mode Fourier series as given in Eqs.(71) and (72). The situation with a magnetic field is somewhat intermediate, since the magnetic potential is coupled dynamically (63) and by the boundary conditions (56) to the concentration field with its strong gradients. We use a multimode expansion for the magnetic field with a number of modes N_1 which is selected independently of N. For c_0 the modes are antisymmetric in z, while for c_1 symmetric modes are appropriate. The numbers N and N_1 of the contributing modes were taken large enough to ensure that the results are insensitive against a further increase of these numbers. For the parameter values considered here, $N=50$ and $N_1=50$ turned out to be sufficient.

VI. APPROXIMATE ANALYTICAL SOLUTION

In this section we derive an approximate analytical stationary solution, which fits the numerical solution, described above, very well. To get this solution, we make use of the fact that $L \sim 10^{-4}$ is extremely small. Starting with the system of equations (58)-(63), we use the Lorenz representation of the temperature and velocity field (68)-(70) and derive approximate solutions for c_0, c_1, and ϕ_1 avoiding the complicated mode expansion (71)-(73).

Let us first consider Eq. (59). In the stationary case, we can integrate this equation once. With the boundary conditions (65) and (67) we find

$$\frac{w_1 c_1}{2} = L\nabla_z\left[(1+M_2\psi_m)c_0 + (1-M_2)\theta_0\right] - L(1-M_2) \tag{74}$$

Far from the boundaries c_0 and c_1 are $\sim L$. This can easily be seen from the consistency of Eq. (61) with Eq. (74) taking into account that far from the boundaries the derivatives of the functions are small. Thus, in Eq. (74) we can neglect c_0, when we are far from the boundaries. Futhermore, we can neglect $\nabla_z\theta_0$ compared to 1, since its influence is very weak [15]. This latter approximation is good, when the amplitude of the velocity is still small, since θ_0 is the nonlinear term in the Lorenz model. Taking this into account we can get the concentration field far from the boundaries as

$$c_1 = -2L(1-M_2)/w_1. \tag{75}$$

To satisfy the boundary conditions for c_1 and to find the profile of the concentration field near the boundaries one needs to solve the boundary layer problem. The expression (75) diverges close to the boundaries as $1/(z-1/2)^2$ (if the boundary is on $z = 1/2$). Thus, the solution of the boundary layer problem has to behave asymptotically like $1/(z-1/2)^2$ far from the boundary, in order to match with Eq. (75). The boundary layer problem for the concentration field is considered in the Appendix A.

Since the boundary layer depth δ is proportional $L^{1/3}$ (see Appendix A) the contribution of the boundary layers gives only small $\sim L^{1/3}$ corrections to the amplitude equation and the expression (75) can be used with $w_1 = A\cos^2(\pi z)$.

The next step is to calculate the magnetic field potential ϕ_1 from Eq. (63). To do that we split the magnetic potential into two parts, $\phi_1 = \phi_{11} + \phi_{12}$ so that

$$\left(\nabla_z^2 - M_3k^2\right)\phi_{11} = \nabla_z\,\theta_1, \tag{76}$$

$$\left(\nabla_z^2 - M_3k^2\right)\phi_{12} = -\psi_m\nabla_z\,c_1. \tag{77}$$

with the boundary conditions

$$\bar\epsilon\nabla_z\phi_{11} \pm k\phi_{11}|_{z=\pm\frac12} = 0 \tag{78}$$

$$\bar\epsilon(\nabla_z\phi_{12} + \psi_m c_1) \pm k\phi_{12}|_{z=\pm\frac12} = 0 \tag{79}$$

The solution for ϕ_{11} is straightforward and simple when we take the temperature field in the form of Eq. (69),

$$\phi_{11} = \frac{\pi B}{\pi^2+a^2}\left(\sin(\pi z) - \frac{k\sinh(az)}{k\sinh(a/2)+\bar\epsilon a\cosh(a/2)}\right) \tag{80}$$

with $a = \sqrt{M_3}k$. The solution for ϕ_{12} has the form

$$\phi_{12} = M\sinh(az) - \frac{\psi_m}{a}\left(\sinh(az)\int_0^z \cosh(a\xi)c_1'(\xi)d\xi - \cosh(az)\int_0^z \sinh(a\xi)c_1'(\xi)d\xi\right) \tag{81}$$

with M a constant of integration. Note that $\phi_{12}(z)$ has to be an antisymmetric function in z. To find M we consider the boundary condition (79). This is done in Appendix B with the final result

$$\phi_{12}(z) = \alpha(1-M_2)\left(\frac{L^2}{\pi^4A^2(1+\psi_mM_2)}\right)^{1/3} \times\frac{k\psi_m}{k\sinh(a/2)+\bar\epsilon a\cosh(a/2)}\sinh(az) + O(L), \tag{82}$$

where $\alpha = -\int_0^\infty \zeta f'(\zeta)d\zeta \approx 2.791$ is a real number of order 1 independent of any parameter of the problem, and the function $f(\zeta)$ is defined in Eq. (A7) in Appendix A.

Having found an approximate expression for the profiles of the concentration and magnetic potential we substitute them into Eq. (59) and then project this equation on the weight function $\cos^2(\pi z)$. Equations (61) and (62) are to be projected with the weight functions $\sin(2\pi z)$ and $\cos(\pi z)$, respectively. This leads to a system of three algebraic equations for the amplitudes A, B, G, [Eq. (68)-(70)], from which we get the final (implicit) expression for the saturation amplitude A as a function of the parameters of the problem:

$$\frac{18\pi^4}{Ra} = \frac{1+M_1(\eta-2\pi\bar\eta G)}{1+3A^2/40\pi^2} + (1-M_2)\frac{32\pi^2}{3A^2}\left[L(\psi+M_1\psi_m) + \gamma(1-\bar\gamma G)M_1\psi_m\left(\frac{L^2A}{1+\psi_mM_2}\right)^{1/3}\right] \tag{83}$$

Here

$$\eta = 1 - \frac{\pi^2}{\pi^2+a^2} + \frac{3\pi^5\sinh(a/2)}{(\pi^2+a^2)(4\pi^2+a^2)(\pi\sinh(a/2)+\bar\epsilon a\cosh(a/2))}, \tag{84}$$

$$\bar\eta = \frac35(1-\frac{\pi^2}{\pi^2+a^2}) + \frac{\pi^2}{\pi^2+a^2}\frac{a}{(\pi\sinh(a/2)+\bar\epsilon a\cosh(a/2))}\frac{3\pi^3(8\pi^2-a^2)\sinh(a/2)}{a(a^4+20a^2\pi^2+64\pi^4)}, \tag{85}$$

$$\gamma = \alpha \frac{2\pi^{5/3}\sinh(a/2)}{(a^2+4\pi^2)(\pi\sinh(a/2)+\bar{\epsilon}a\cosh(a/2))}, \quad (86)$$

$$\bar{\gamma} = \pi - \frac{3\pi a^2}{a^2+16\pi^2}. \quad (87)$$

G, the stationary amplitude of θ_0 Eq. (70), is

$$G = \frac{9A^2}{160\pi^3(1+3A^2/40\pi^2)}, \quad (88)$$

while $B = (5\pi^2/2A)G$. In Eq. (83) we have chosen $k = \pi$ in order to simplify the formula. This is reasonable, since the wave number of the maximum growth k_c is close to π. The second term on the right of Eq. (83) can be seen as an expansion in $\psi_m L^{2/3}$ and ψL. Since the prefactor of the former is quite small, we have also kept the leading contribution to order $\psi_m L$. The complete evaluation of the $\psi_m L$ term is hardly worth doing, since it makes formula (83) unnecessary complicated without significantly changing the quantitative results. The occurrence of fractional powers of A^2 and L as products with ψ_m and M_1 indicates the importance of the boundary layers in the case of an external field.

VII. INFLUENCE OF THE KELVIN FORCE

We first investigate the influence of the Kelvin force on the convection and disregard magnetophoresis for the moment by putting $M_2 = 0$. The equations for the mode amplitudes A, B, G, a_n, and b_n have been solved by a Runge-Kutta integration. The wave number k, usually taken to characterize the mode of maximum linear growth rate $\lambda(k, Ra)$, varies between 3 and 3.5 within the Rayleigh number regime investigated. However, since the final predictions of our model turn out not to depend sensitively on the k value chosen, we adopt in all of our simulations $k = 3.1$. All runs are started from the initial configuration of an undisturbed linear temperature and magnetic field profile and a constant concentration as given in Eqs. (36) - (38), and small random velocity fluctuations to start the convection process.

In all of our runs the convective motion was found to settle into a stationary convection in the same way as it is in the absence of magnetic field [3]. There are roughly three different regimes of time evolution: linear growth, nonlinear transition to a saturation state, and the saturation state itself. When we fix the temperature gradient (i.e., take the Rayleigh number constant) and change the magnetic field strength, we have the bifurcation picture as a function of M_1. This is the most convenient bifurcation curve to compare with experiment, since during experiments it is much easier to change M_1 (i.e. the magnetic field) than the Rayleigh number (i.e. the temperature difference). This bifurcation diagram is shown in Fig. 1 for different values of the separation ratios ψ and ψ_m. These two parameters are related to the two different mechanisms of how the concentration inhomogeneity changes the bifurcation picture. The separation ratio ψ is independent of the magnetic nature of the grains and describes the concentration buoyancy force due to the density difference of the solvent liquid and the magnetic grains. The second mechanism is due to the Kelvin force, which arises from the concentration variations of the magnetic particles and the resulting strong variations of the magnetic susceptibility. This effect relies on the magnetic nature of the ferrofluid particles and is characterized by the magnetic separation ratio ψ_m.

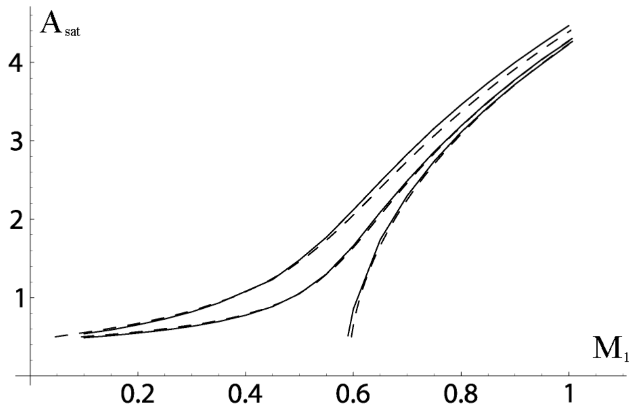

FIG. 1: The saturation amplitude $A_{sat} = A(t \to \infty)$ as a function of M_1 at $Ra = 1300$ for different values of ψ and ψ_m (see text). The dashed lines are the analytical result (83).

Without any concentration variations ($\psi_m = 0$ and $\psi = 0$) we have the usual pitchfork bifurcation with respect to M_1 (Fig. 1). If only the nonmagnetic mechanism is switched on ($\psi = 10$, $\psi_m = 0$), the bifurcation looks like an imperfect one with a nonzero saturation amplitude even in the subcritical parameter range. In the supercritical parameter range the amplitude approaches that of the homogeneous ferrofluid. If we additionally switch on the magnetic buoyancy effect ($\psi_m = 10$), the bifurcation deviates strongly from the previous cases and, in particular, has a different saturation behavior for strong magnetic fields. We should point out that in order to get this numerical result at least 50 modes each for the concentration and magnetic field have to be taken into account. Comparing this to the case without a magnetic field [3], when 20 modes were more than enough, we can see the importance of the boundary layers when the magnetic field is on. In Fig. 1 the analytical results, Eq. (83), are shown as dashed lines. The agreement between the numerical and analytical result is very good.

VIII. INFLUENCE OF MAGNETOPHORESIS

In this section we discuss the influence of magnetophoresis ($M_2 \neq 0$). In the implicit equation for the amplitude, Eq. (83), the magnetophoretic effect is manifest in two different ways. First, there is the global prefactor $(1 - M_2)$ in the second term and, second, there is the denominator $(1 + M_2\psi_m)^{1/3}$ in the term proportional to $L^{2/3}$. Since M_2 is negative but $M_2\psi_m > -1$ [cf. the discussion after Eq. (44)] both effects grow with the external field.

The second effect gets very pronounced, when the product $M_2\psi_m$ approaches its stability limit -1. This happens for a magnetic field $H_0 \to H_c$ with $H_c^2 = \gamma_H \bar{\epsilon}\,\chi_c^{-2}$, where, however, the susceptibilities may themselves be (weak) functions of H_0^2 for strong fields. In that limit the boundary layer becomes singular, which is indicated in the numerical approach by the necessity to take into account more and more spatial modes. The analytical treatment also breaks down and Eq.(83) is no longer a good description. The breakdown of thermodynamic stability also shows up in the diffusion equation for the concentration

$$\partial_t c(z,t) = L(1+\psi_m M_2)\partial_z^2 c(z,t) \tag{89}$$

that follows from Eqs. (41) and (43) under the assumption that the temperature equilibrates much faster. For $H_0 \to H_c$ the diffusional time scale diverges and, therefore, the boundary layer profile gets sharper. This can also be inferred from the Eq. (A9), which shows the boundary layer depth to scale with $[L(1+\psi_m M_2)]^{1/3}$. For the amplitude the effect of M_2 is very weak and hardly visible in a plot like Fig. 1, except for the immediate vicinity of the stability limit $(1 + M_2\psi_m) = 0$.

The breakdown of thermodynamic stability may be related to particle agglomeration and internal structure formation. The magnetophoretic effect is due to the force that drives magnetic particles to areas of larger magnetic field strength. This leads to agglomerations where the magnetic field is larger and consequently attracts further particles. This mechanism is compensated by the (magnetic field independent) diffusive motion of the particles. When the strength of the magnetic field exceeds a certain value, the diffusion fails to prevent agglomeration of the particles and structures are built. In that case a description in terms of an ordinary binary mixture is no longer possible.

IX. CONCLUSION

We have derived the complete set of equations to describe ferrofluids in an external magnetic field in terms of a binary mixture. Magnetophoretic effects as well as magnetic stresses have been taken into account in the static and dynamic parts of the equations. They were used to investigate the thermal convection instability of ferrofluids in the presence of an external magnetic field. As in the case without a magnetic field, the effect of the concentration field is manifest in an apparent imperfection of the bifurcation. A magnetic field makes this imperfection more prononced. More important, however, not only does an external magnetic field lead to pronounced boundary layer profiles (with respect to the concentration and magnetic potential), this boundary layer also couples effectively to the bulk behavior due to the magnetic boundary condition. This makes the numerical solution of the bifurcation problem considerably more complicated than without a magnetic field. Nevertheless, we were able to present an approximate analytical solution by taking explicitly into account part of the boundary layer behavior. The agreement between the analytical and the numerical solutions was very good. We also discuss the limitations of the binary mixture model. In a strong external field diffusion fails to prevent agglomeration of the particles due to magnetophoresis. In that case the breakdown of the binary mixture model shows up by the occurrence of a negative effective diffusion constant.

ACKNOWLEDGMENTS

Helpful discussions with M. Lücke are gratefully acknowledged. This work is supported by "Schwerpunktprogramm 1104 Colloidal Magnetic Fluids" of the Deutsche Forschungsgemeinschaft.

APPENDIX A: THE BOUNDARY LAYER PROBLEM

We consider Eqs. (60), (74), and (79) in the vicinity of the boundary $z = 1/2$. Near the boundary the derivatives with respect to z of the functions c_0, c_1, and ϕ are large and we use this fact to simplify these three equations as

$$\frac{1}{2}\,(w_1 c_1) \;=\; L(1+M_2\psi_m)c_0' - L(1-M_2), \tag{A1}$$

$$w_1 c_0' \;=\; L\left(c_1'' - M_2\,\phi_{12}'''\right), \tag{A2}$$

$$\phi_{12}'' \;=\; -\psi_m c_1', \tag{A3}$$

under the assumptions

$$\phi_{11}''' \ll \phi_{12}''' \quad \text{and} \quad \nabla_z^2 \gg \mathrm{k}^2, \tag{A4}$$

Combining these three equations into one we get an equation for c_1

$$\frac{1}{2} w c_1 = \frac{L^2(1+M_2\psi_m)^2}{w} c_1'' - L(1-M_2). \tag{A5}$$

Near the boundary $z = -1/2$ we have $\varepsilon = z - 1/2 \ll 1$. Expanding $\cos^2(\pi z)$ in powers of ε the velocity $w_1 = A\pi^2\varepsilon^2$ and Eq. (A5) takes the form

$$\frac{\pi^2 A}{2L(1-M_2)}\varepsilon^4 c_1 = \frac{L(1+M_2\psi_m)^2}{\pi^2 A(1-M_2)} c_1'' - \varepsilon^2. \tag{A6}$$

We rescale the concentration field and z coordinate in such a way that the final equation becomes independent of any parameters and appears to be a universal equation defining the boundary layer profile

$$\frac{1}{2}\zeta^4 f + \zeta^2 = f'', \tag{A7}$$

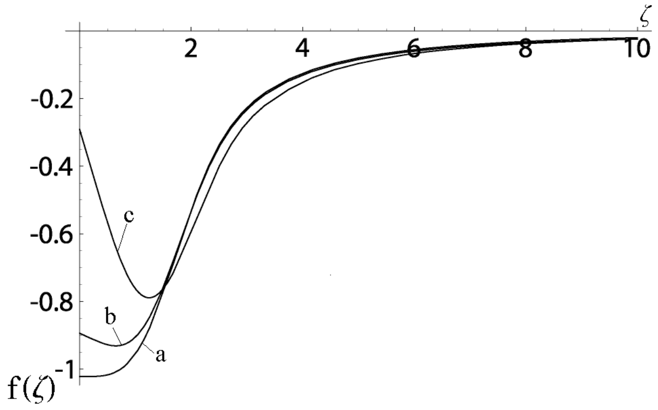

FIG. 2: The boundary layer profiles obtained from (a) the analytical solution $f(\zeta)$, Eq. (A7),(b) the multimode numerical solution scaled with Eq. (A9) for $M_1 = 0.1$, and (c) for $M_1 = 1.0$ ($M_2 = 0$, $\psi = 10$, and $\psi_m = 10$).

with

$$\zeta = \left(\frac{\pi^2 A}{L(1+\psi_m M_2)}\right)^{1/3} \varepsilon, \tag{A8}$$

$$c_1(z) = (1 - M_2)\left(\frac{L}{\pi^2 A(1+\psi_m M_2)^2}\right)^{1/3} f(\zeta). \tag{A9}$$

Thus, the layer depth δ scales with $L^{1/3}$. We assume that the boundary condition (64) for the concentration field c_1 can be replaced by a homogeneous one $c_1'(\pm 1/2) = 0$ leading to $f'(0) = 0$. In this case the boundary layer profile becomes self-similar. As a second boundary condition we require that the function $f(\zeta)$ has the asymptotic form $f(\zeta) \to -2/\zeta^2$ when $\zeta \to \infty$, in order to be compatible with the bulk solution (75). In Fig. 2 we compare the boundary layer profiles that follow from the analytical solution (A7)–(A9) with those obtained numerically. The approximaton $f'(0) = 0$ is good when M_1 is not too large, e.g., for $M_1 = 0.1$ the agreement between numerics and analytics is better than for $M_1 = 1.0$. The important quantity we extract from the boundary layer considerations and that enters Eq. (83) is $\alpha = \int_0^\infty \xi f'(\xi) d\xi$. The error made by calculating this number using the condition $f'(0) = 0$ is of the order of 30% when compared with the numerical result for $M_1 = 1.0$, where $f'(0) \approx -0.5$ (Fig. 2). This correction would change the analytically determined amplitudes [Eq. (83) in Fig. 1] by only about 1%.

APPENDIX B: CALCULATION OF THE MAGNETIC FIELDS ϕ_{12}

To satisfy the boundary conditions for the magnetic potential we need to substitute the expression (81) into Eq. (79). Doing so we get integrals of the type

$$\int_0^{1/2} \cosh(a\xi) c_1'(\xi) d\xi, \quad \int_0^{1/2} \sinh(a\xi) c_1'(\xi) d\xi, \tag{B1}$$

which would diverge, if we simply used expression (75) for the concentration field. To resolve these singularities we have solved the boundary layer problem for the concentration field in the preceding section. Let us consider the first integral; the second one is treated in the same way. We can divide this integral into two parts:

$$\int_0^{1/2} \cosh(a\xi) c_1'(\xi) d\xi = \int_0^{1/2-\Delta} \cosh(a\xi) c_1'(\xi) d\xi + \int_{1/2-\Delta}^{1/2} \cosh(a\xi) c_1'(\xi) d\xi. \tag{B2}$$

Here Δ is a small but fixed value, chosen in such a way that for $z > \Delta$ the bulk profile (75) and for $z < \Delta$ the boundary layer profile (A9) are valid. In the second integral we can expand $cosh(a\xi)$ in the vicinity of $\xi = 1/2$. Then we can write

$$\begin{aligned} \int_{1/2-\Delta}^{z} \cosh(a\xi) c_1'(\xi) d\xi &= \cosh\left(\frac{a}{2}\right) \int_{1/2-\Delta}^{z} c_1'(\xi) d\xi \\ &\quad + a \sinh(\frac{a}{2}) \int_{1/2-\Delta}^{z} (\xi - 1/2) c_1'(\xi) d\xi + \ldots \\ &\equiv \cosh\left(\frac{a}{2}\right) I_0(z) + a \sinh\left(\frac{a}{2}\right) I_1(z) \\ &\quad + \frac{a^2}{2} \cosh\left(\frac{a}{2}\right) I_2(z) + \ldots \end{aligned} \tag{B3}$$

for $z \to 1/2$. Since c_1' is regular at the boundary and the boundary layer depth $\delta \sim L^{1/3}$, the expansion (B3) is actually an expansion in powers of $L^{1/3}$.

If we substitute the expression (B3) [and the appropriate one for the second integral in Eq. (B1)] into the potential ϕ_{12} (81), the boundary condition (79) for $z = 1/2$ takes the form

$$\begin{aligned} M\left(k \sinh(\frac{a}{2}) + \bar{\epsilon} a \cosh(\frac{a}{2})\right) + k\psi_m I_1(z \to 1/2) \\ + \bar{\epsilon}\left[-I_0(z \to 1/2) + c(1/2)\right] + \ldots = 0 \end{aligned} \tag{B4}$$

where the ellipsis indicates terms of O(L), e.g., $I_2(z \to 1/2)$. From the definition of $I_0(z)$ we can see that the leading contributions in the brackets cancel and only terms $\sim L^{2/3}$ are left. Thus, the main contribution to M is proportional to the integral $I_1(z \to 1/2)$,

$$M = -\frac{k\psi_m}{k \sinh(\frac{a}{2}) + \bar{\epsilon} a \cosh(\frac{a}{2})} I_1(z \to 1/2). \tag{B5}$$

With the expression (A9) we can calculate the integral $I_1(z \to 1/2)$

$$I_1(z \to 1/2) \ = \ \int_{1/2-\Delta}^{1/2} (\xi - 1/2) c_1'(\xi) d\xi = -(1-M_2) \left(\frac{L^2}{\pi^4 A^2 (1+\psi_m M_2)} \right)^{1/3} \int_0^\infty \zeta f'(\zeta) d\zeta + O(L), \qquad \text{(B6)}$$

where we have replaced Δ as the upper limit of the integral by ∞. The error introduced is canceled by the first integral of Eq. (B2), (which we have not considered so far,) if the bulk and boundary-layer concentration fields c_1 are matched at $z = \Delta$. Since in the bulk $c_1 \sim L$, the remaining contribution of the first integral in Eq. (B2) is of O(L), which we neglect. Finally, the magnetic field ϕ_{12} in the bulk of the layer takes the form

$$\phi_{12}(z) = \alpha (1-M_2) \left(\frac{L^2}{\pi^4 A^2 (1+\psi_m M_2)} \right)^{1/3} \frac{k\psi_m}{k \sinh(a/2) + \bar{\epsilon} a \cosh(a/2)} \sinh(az) + O(L), \qquad \text{(B7)}$$

where $\alpha = \int_0^\infty \zeta f'(\zeta) d\zeta \approx 2.791$ is a real number independent of any parameter of the problem.

[1] R. E. Rosensweig, *Ferrohydrodynamics* (Cambridge University Press, England Cambridge 1985).
[2] E. Blums, A. Mezulis, M. Maiorov, and G. Kronkalns, J. Magn. Magn. Mater. **169** 220 (1997).
[3] A. Ryskin, H.-W. Müller, and H. Pleiner, Phys. Rev. E **67** 046302 (2003).
[4] H. Pleiner and H. R. Brand, in *Pattern Formation in Liquid Crystals*, edited by A. Buka and L. Kramer (Springer, NewYork, 1996), Chap. 2.
[5] E. Jarkova, H. Pleiner, H.-W. Müller, A. Fink, and H. R. Brand, Eur. Phys. J. E **5**, 583 (2001).
[6] A. Ryskin, H. Pleiner, and H.-W. Müller, Eur. Phys. J. E **11**, 389 (2003).
[7] We use rationalized Gaussian (or Heaviside-Lorentz) units. For a conversion to standard SI units, see J.D. Jackson, *Classical Electrodynamics*, 2nd ed. (Wiley, New York 1975).
[8] With the usual heuristic definition $\chi = \partial M / \partial H$ there is $\chi = \chi_0 + \chi_H H_0^2$ and $\bar{\epsilon} = 1 + \chi$.
[9] A. Recktenwald and M. Lücke, J. Magn. Magn. Mater. **188** 326 (1998).
[10] B. A. Finlayson, J. Fluid Mech. **40** 753 (1970).
[11] G. K. Auernhammer and H. R. Brand, Eur. Phys. J. B **16** 157 (2000).
[12] J. Lenglet, A. Bourdon, J.-C. Bacri, and G. Demouchy, Phys. Rev. E **65** 031408 (2002).
[13] E. N. Lorenz, J. Atmos. Sci. **20** 130 (1963).
[14] In the simplest case this is a five-mode model for $A_1 = A_0(2+k)$ and $A_n = 0$ for $n \geq 2$.
[15] S. Hollinger, M. Lücke, and H.-W. Müller, Phys. Rev. E **57** 4250 (1998).